

Supplement

Table of Contents

Supplement	1
S1. Sample collection and storage	2
S2. DNA Extraction	2
S3. Next generation DNA sequencing	2
S4. Positive and negative controls	2
S5. Sequence analysis and quality control	3
S6. qPCR to determine microbial load in DFUs from swabs	3
S7. Characterization and visualization of DFU biofilm.....	3
S8. Scanning electron microscopy (SEM) and peptide nucleic acid fluorescent in situ hybridization (PNA-FISH) with confocal laser scanning microscopy (CLSM) sample preparation and image interpretation	4
S9. Total microbial load of DFUs – individual patient data. Baseline (week 0), mid-point (week 3) and end of treatment (week 6).	6
10. Wound metrics captured at baseline and end of treatment (EOT).....	8
11. SEM and PNA-FISH. Additional images for reference.....	9

S1. Sample collection and storage

All DFUs were debrided and cleansed with NaCl 0.9% prior to specimen collection. For qPCR and DNA sequencing, ulcer specimens using swabs (Puritan®, Zymo DNA/RNA shield™, Zymo Research, Irvine, CA, USA) were obtained using the Levine technique by pressing firmly onto the wound bed and rotating the sterile swab head onto the wound bed. Swabs were refrigerated at 4° for 24 hours and then stored at -80°C. For SEM and PNA-FISH, tissue specimens were obtained through a dermal ring curette from the wound bed of each DFU. Following removal, tissue specimens were rinsed vigorously in a phosphate buffer solution (PBS) bath to remove any coagulated blood and to reduce the number of planktonic microorganisms. Tissue specimens for PNA-FISH were immediately fixed in 4% paraformaldehyde overnight at 4°C, then transferred into 70% ethanol and stored at -20°C. Tissue specimens for SEM were immediately fixed in 3% glutaraldehyde overnight at 4°C, then transferred into 0.1% phosphate buffer (PB) and stored at -80°C. All tissue samples remained in storage until study completion to reduce any bias and were processed in bulk. Participant identifiers and group allocation were not disclosed to the scientist undertaking the analyses

S2. DNA Extraction

Swabs obtained from DFUs were defrosted on ice prior to DNA extraction. Genomic DNA was extracted using Qiagen DNeasy PowerBiofilm kit (Cat No./ID: 24000-50) following the manufacturer's instructions.

S3. Next generation DNA sequencing

Preparation of the 16S library and DNA sequencing was carried out by a commercial laboratory (Ramaciotti Centre for Genomics, University of New South Wales, Australia) on the Illumina MiSeq platform (2x300bp) targeting the V1-V3 (27f/519r) 16S region.

S4. Positive and negative controls

Positive and negative controls were utilised during sequencing and microscopy. For sequencing, positive controls were performed using the ZymoBIOMICS Microbial Community Standard (Zymo Research, Irvine, CA, USA) and negative controls were performed using Milli-Q® ultrapure water. Sequencing of controls revealed no contamination of samples. For PNA-FISH, a loop full of overnight cultures of *S. aureus* (ATCC® 35556™) and *Pseudomonas aeruginosa* (ATCC® 15692™) were grown overnight (37°C, 180 rpm) in 5 mL of tryptic soy broth (TSB) or lysogeny broth (LB) media, respectively. One loopful of each

was then smeared into one drop of fixation solution (AdvanDX, Woburn, USA) and incubated at 65°C on a heating block until dry.

S5. Sequence analysis and quality control

16S rRNA gene amplicons were processed using the QIIME2 pipeline¹ as follows; denoising of reads was completed using Deblur² with a trim length of 240bp, which merged reads and removed chimeric sequences and reads with ambiguous bases. From 11,304,249 sequences, 661 sOTUs were calculated by Deblur with a total frequency of 6,050,631. Taxonomy was assigned to sOTUs using VSEARCH3 against the SILVA database (v132)⁴. Prior to statistical analysis, samples were rarefied to 3761 reads per sample to ensure even sampling depth. Bray-Curtis dissimilarity, species richness and Shannon's diversity index⁶ were calculated and visualized using the diversity plugin of QIIME2.¹ Data was then imported to R using Qiime2R⁷ for the generation of all plots.

S6. qPCR to determine microbial load in DFUs from swabs

qPCR was utilized to quantify the total microbial load present within DFU swab samples as described by Kalan et al. Briefly, the reaction was prepared by mixing the Taqman Fast Advanced Master Mix (2x) (ThermoFisher Scientific, Waltham, MA, USA), Taqman 16S Gene Expression Assay (20x) (ThermoFisher Scientific, Waltham, MA, USA), nuclease free water and 50ng of template in a total volume of 10 or 20 uL. The reaction was then run on a Quantstudio 7 Flex Real Time PCR system (ThermoFisher Scientific, Waltham, MA, USA) using the following conditions; 95°C for 2 min, followed by 40 cycles of 95°C for 1 sec and 60°C for 20 sec. A set of standards ranging from 2000 pg to 1.95 pg were included and used to generate a standard curve for determining the amount of 16S product within the DFU swab samples. Total bacterial load was then determined using the equation $[10^{LC}] * 200$ where LC is the log concentration of 16S product, followed by multiplying the result by the total extraction volume.

S7. Characterization and visualization of DFU biofilm

The presence or absence of biofilms in chronic non-healing DFUs, was confirmed through SEM or PNA-FISH with CLSM. For the purpose of this study, we used definitions promoted by an expert group to characterise biofilm as being; microbial aggregates surrounded by a self-produced or host derived matrix adhering to natural or artificial surfaces in the host, or aggregates associated with but not directly adherent to the surface.¹⁰

S8. Scanning electron microscopy (SEM) and peptide nucleic acid fluorescent in situ hybridization (PNA-FISH) with confocal laser scanning microscopy (CLSM) sample preparation and image interpretation

In vivo microbial biofilms associated with DFU tissue were sampled at 5–200 μm for optimal visualisation through scanning electron microscopy.¹¹ 2-3 millimetres of DFU tissue were fixed in 3% glutaraldehyde, followed by 3 washes of 0.1M phosphate buffer prior to serial ethanol dehydration and processing in a CPD300 Critical Point Dryer (Leica) for 20 cycles to retain the original structure of the tissue. Dried samples were coated with 20-nm gold film and examined using a Zeiss GeminiSEM at a WD of 5-7mm and 7.00 kV. Tissue specimens were scanned for microbial aggregates and extracellular polymeric substances (EPS) by orientating the specimen to the wound bed surface side of the tissue, then working in a zigzag pattern at magnifications ranging from 300X to approximately 5,500X. Each sample was scored based on the amount of bacteria/biofilm observed using an arbitrary five-point scale as previously reported.¹² Score 0 = no bacteria observed; score 1 = single individual cells; score 2 = small micro-colonies (~ 10 cells); score 3 = large micro-colonies (~100 cells); score 4 = continuous film; score 5 = thick continuous film.

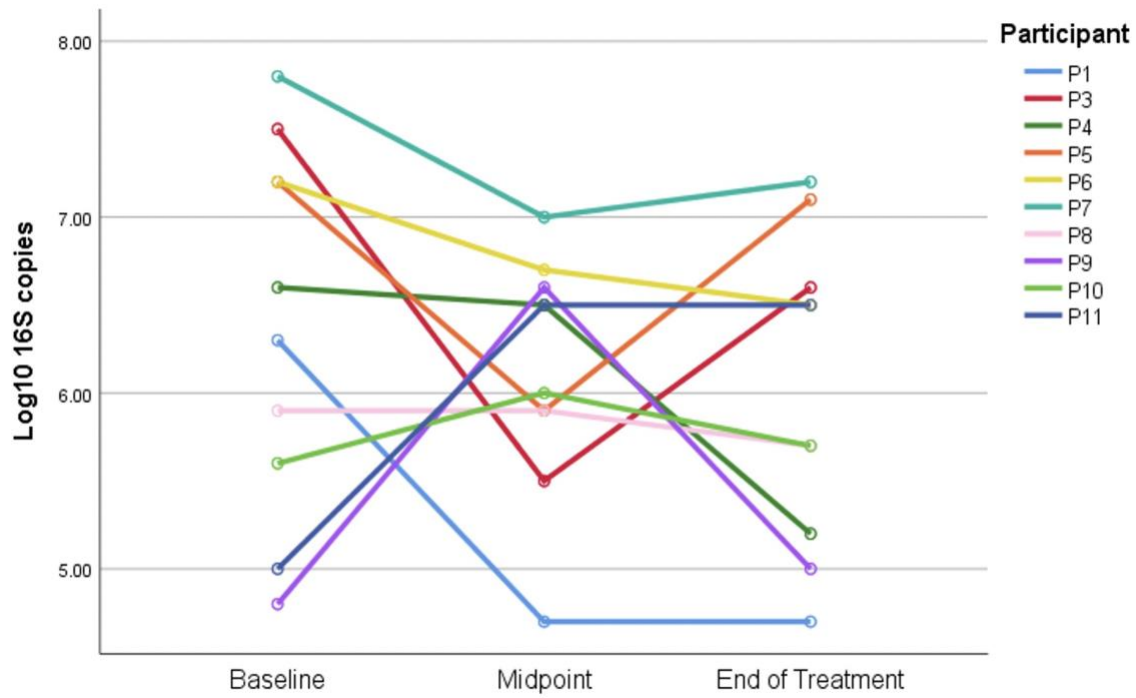
For CLSM, the tissue was fixed in 4% Paraformaldehyde prior to processing and paraffinization using an Excelsior ES tissue processor (ThermoFisher Scientific, Waltham, MA, USA). Tissue sections were then cut at 4 microns and deparaffinised using sequential washes with Xylene and decreasing concentrations of ethanol. Dried sections were then stained with the BacUni TXR probe (AdvanDX, discontinued) for 90 min at 55°C followed by a 30 min wash in 1X wash buffer at 55°C (AdvanDX). 0.3mM DAPI was then added as a counterstain for 15 min. Specimens were then visualized by an experienced laboratory scientist on a Zeiss LSM 880 confocal microscope using a 63x oil immersion objective. Two adjacent sections were observed per sample. Sections were thoroughly reviewed by scanning side-to-side from top to bottom over each section. Fluorophores were excited by laser excitation at 405 (6-diamidino-2-phenylindole -DAPI), 488 (fluorescein - FLU), or 561 nm (Tyro3, Axl, and Mer -TAM). One image was taken using each excitation wavelength. All post-capture image processing was done in Imaris v8.4 (Bitplane AG, Zurich, Switzerland). All viewing authors (MR, SS, MM) were experienced in viewing biofilm architecture and reached a consensus about the presence of biofilm in each sample.

References for Methods:

1. Caporaso JG, Lauber CL, Walters WA, Berg-Lyons D, Huntley J, Fierer N. et al. Ultra-high-throughput microbial community analysis on the Illumina HiSeq and MiSeq platforms. *ISME Journal* 2012; 6:1621-1624.
2. Amnon Amir, Daniel McDonald, Jose A Navas-Molina, Evguenia Kopylova, James T Morton, Zhenjiang Zech Xu, Eric P Kightley, Luke R Thompson, Embriette R Hyde, Antonio Gonzalez, and Rob Knight. Deblur rapidly resolves single-nucleotide community sequence patterns. *MSystems*, 2(2):e00191–16, 2017.
3. Bokulich NA, Kaehler BD, Rideout JR, Dillion M, Bolyen E, Knight R. et al, Optimizing taxonomic classification of marker-gene amplicon sequences with QIIME 2's q2-feature-classifier plugin. *Microbiome* 2018; 6: 1-17.
4. Quast, Christian et al. “The SILVA ribosomal RNA gene database project: improved data processing and web-based tools.” *Nucleic acids research* vol. 41, Database issue (2013): D590-6.
5. Sorensen TA. A method of establishing groups of equal amplitude in plant sociology based on similarity of species content and its application to analyses of the vegetation on Danish commons. *Biol Skar* 1948; 5: 1-34.
6. Shannon CE, Weaver W. The mathematical theory of communication. *University of Illinois Press* 1949. Champaign, Illinois.
7. qiime2R: Importing QIIME2 artifacts and associated data into R sessions. Jordan E Bisanz (2018) <https://github.com/jbisanz/qiime2R>.
8. Hu H, Jacombs A, Vickery K, Merten SL, Pennington DG, Deva AK. Chronic Biofilm Infection in Breast Implants Is Associated with an Increased T-Cell Lymphocytic Infiltrate: Implications for Breast Implant–Associated Lymphoma. *Plast Recon Surg* 2015; 135: 319-29.
9. Jacombs A, Allan J, Hu H, et al. Prevention of Biofilm-Induced Capsular Contracture With Antibiotic-Impregnated Mesh in a Porcine Model. *Aesth Surg J* 2012; 32: 886-91.
10. Høiby N, Bjarnsholt T, Moser C, et al. ESCMID guideline for the diagnosis and treatment of biofilm infections 2014. *Clin Microbiol Infec* 2015; 21: S1-S25.
11. Bjarnsholt T, Alhede M, Alhede M, et al. The in vivo biofilm. *Trends Microbiol* 2013; 21(9): 466-74.

12. Han A, Zenilman JM, Melendez JH, et al. The importance of a multifaceted approach to characterizing the microbial flora of chronic wounds. *Wound Repair Regen* 2011; 19: 532-41.

S9. Total microbial load of DFUs – individual patient data. Baseline (week 0), mid-point (week 3) and end of treatment (week 6).



Log10 16S copies for each individual.

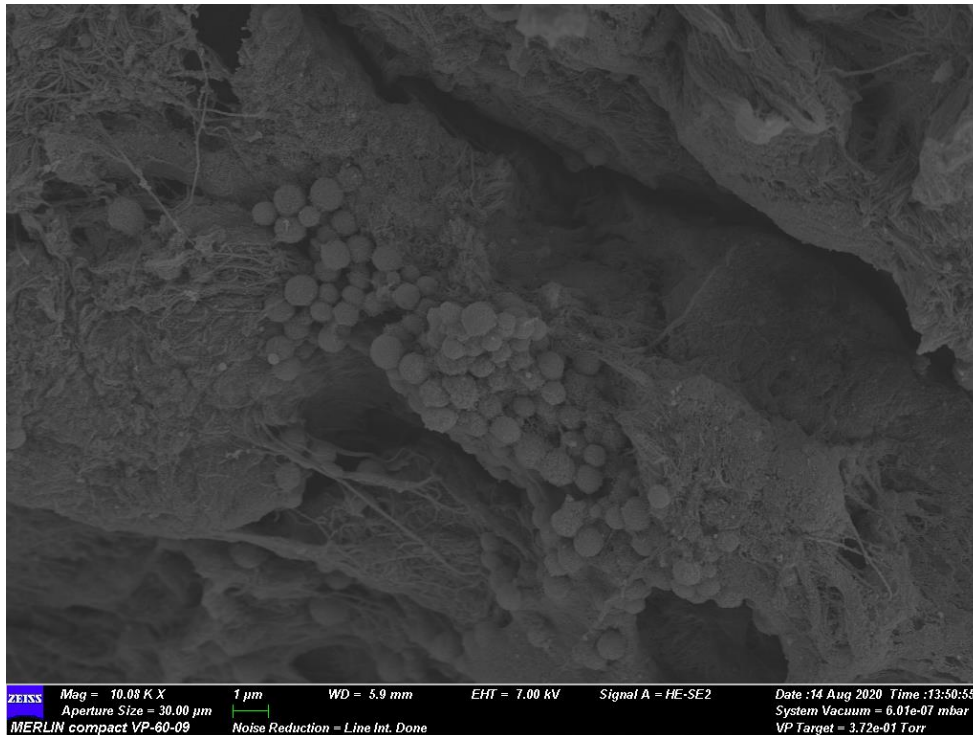
	P1	P3	P4	P5	P6	P7	P8	P9	P10	P11
Baseline	6.3	7.5	6.6	7.2	7.2	7.8	5.9	4.8	5.6	5
Mid-point	4.7	5.5	6.5	5.9	6.7	7	5.9	6.6	6	6.5
End of Treatment	4.7	6.6	5.2	7.1	6.5	7.2	5.7	5	5.7	6.5

10. Wound metrics captured at baseline and end of treatment (EOT)

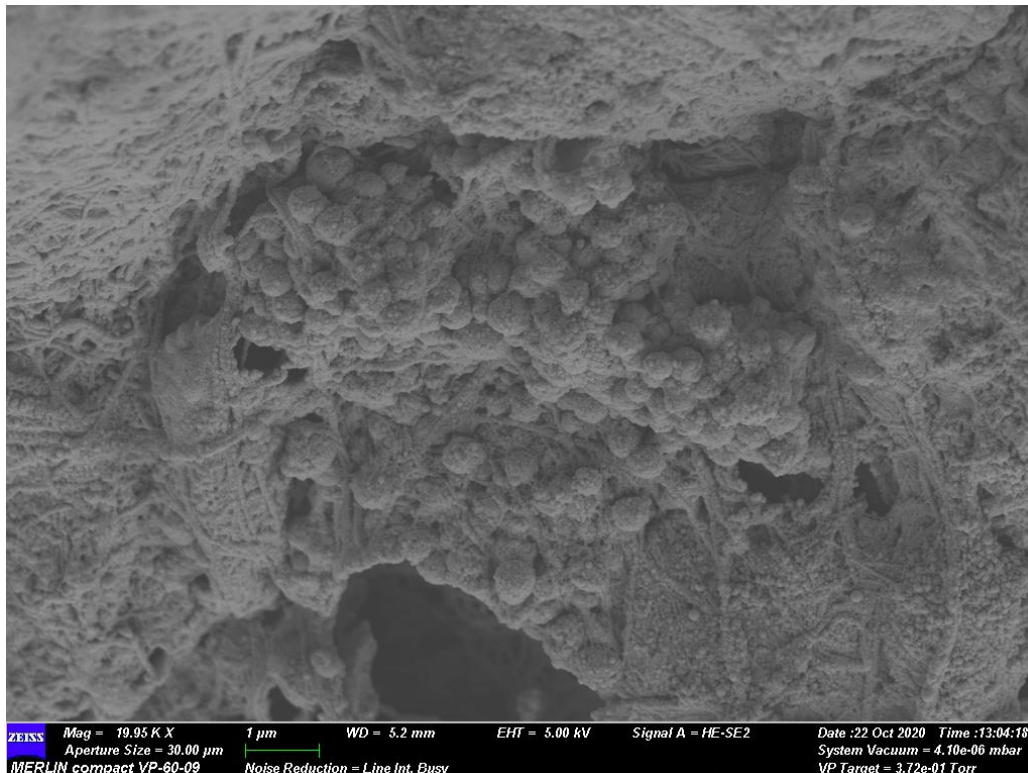
	Ulcer Dimensions				Ulcer Dimensions				Healing or no healing (<10%)	% area size reduction - from baseline to EOT	% depth reduction cumulative from baseline to EOT
	Baseline				End of Treatment						
	Length	Width	Depth	Wound Area (mm2)	Length	Width	Depth	Wound Area (mm2)			
P01	4.9	2.8	0.4	1170	2.7	1.1	0.3	401	1	65.7	25
P02											
P03	2.5	1.7	2.5	310	2.4	1.5	1.1	260	1	16.1	56
P04	2.6	2.8	3	550	2.6	2.7	2.8	530	0	3.6	6.6
P05	2.5	2.1	0.4	370	5	3.5	1.5	450	0	21.6 (increase)	275 (increase)
P06	2.3	2.6	0.2	620	2.1	2.4	0.1	504	1	18.7	50
P07	2.2	1.1	0.3	190	2.2	1.1	0.2	200	0	5.3 (increase)	33.3
P08	4	3	0.1	960	4.2	3.2	0.3	1000	0	4.2 (increase)	200
P09	5.5	3.8	0.1	1170	2.2	1.9	0	280	1	76	100
P10	3.4	5.1	0.1	1333	2.5	4.6	0.1	901	1	32.4	100
P11	4.4	3.7	0.5	1210	3.5	3.4	0.2	860	1	29	60

11. SEM and PNA-FISH. Additional images for reference.

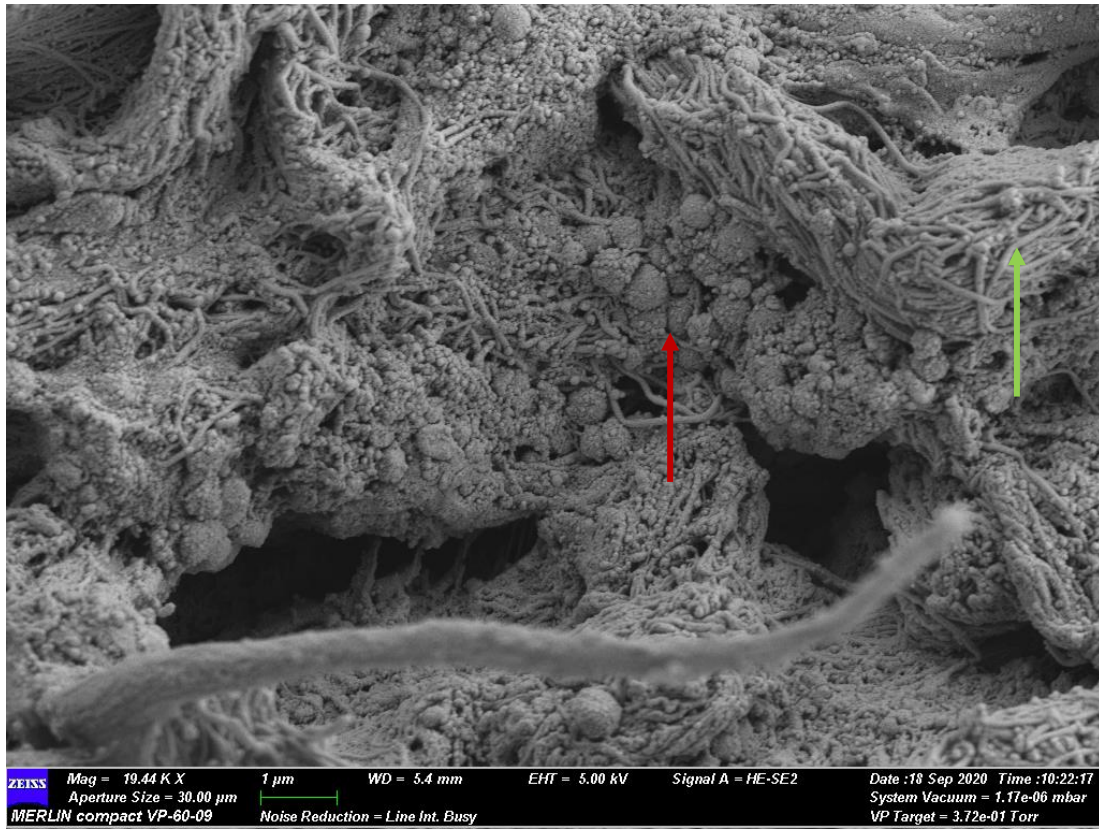
a. Sample P_2. Coccoid aggregates located in a crevice of tissue that was not the immediate surface anatomy.



b. Sample P_8. Coccoid aggregates in a dense extracellular polymeric substance (EPS).



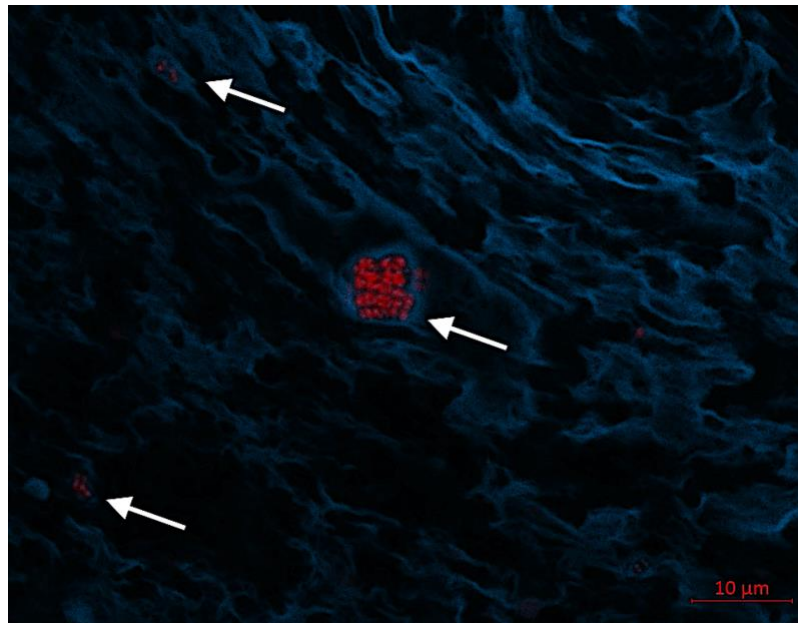
c. Sample P_6. Small aggregates of coccid bacteria (red arrow). Green arrow denotes host material – likely fibrin



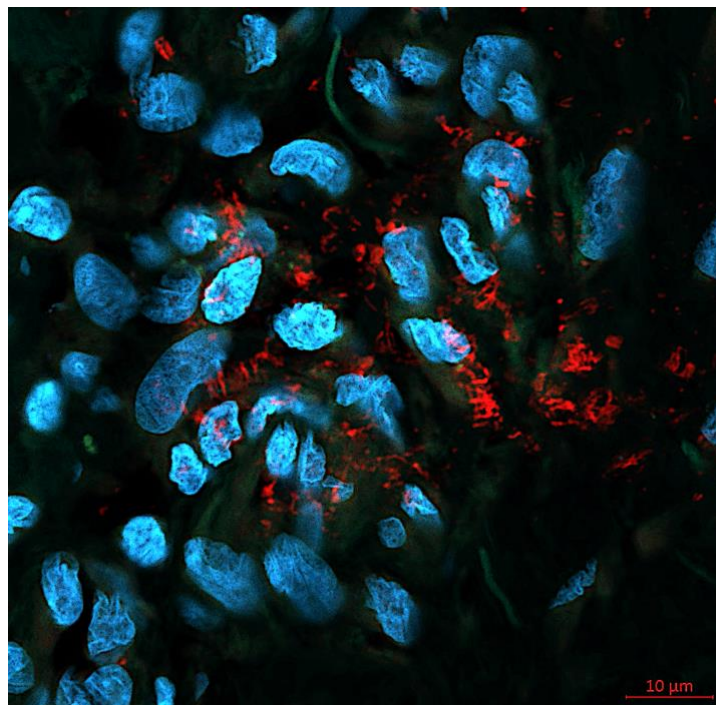
d. Sample P_5. Small aggregate of coccid cells.



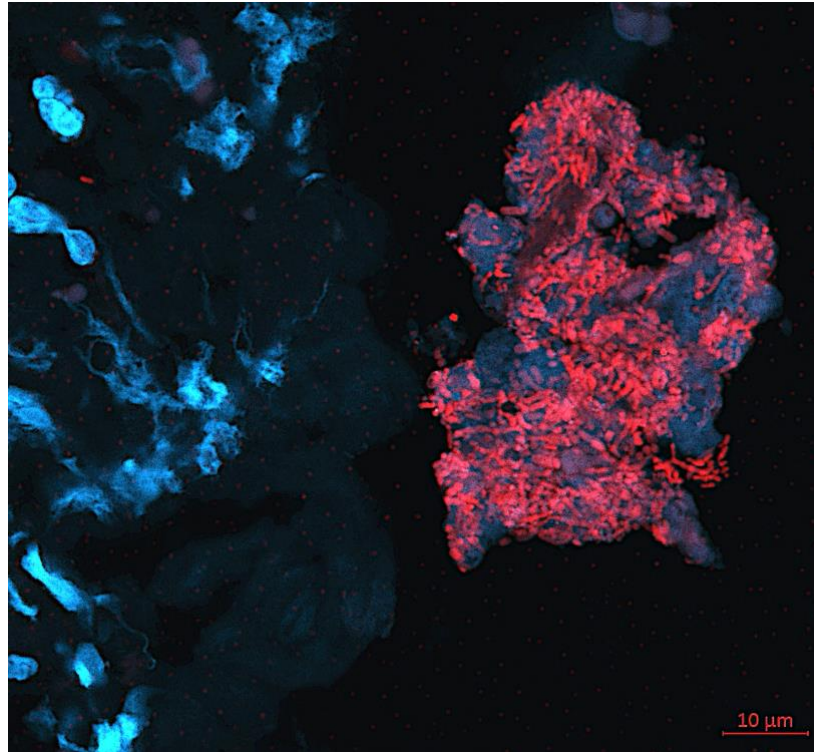
e. Sample P_3. Three separate clusters of microbial aggregates as shown by the arrows. Central, largest cluster with coccoid cells.



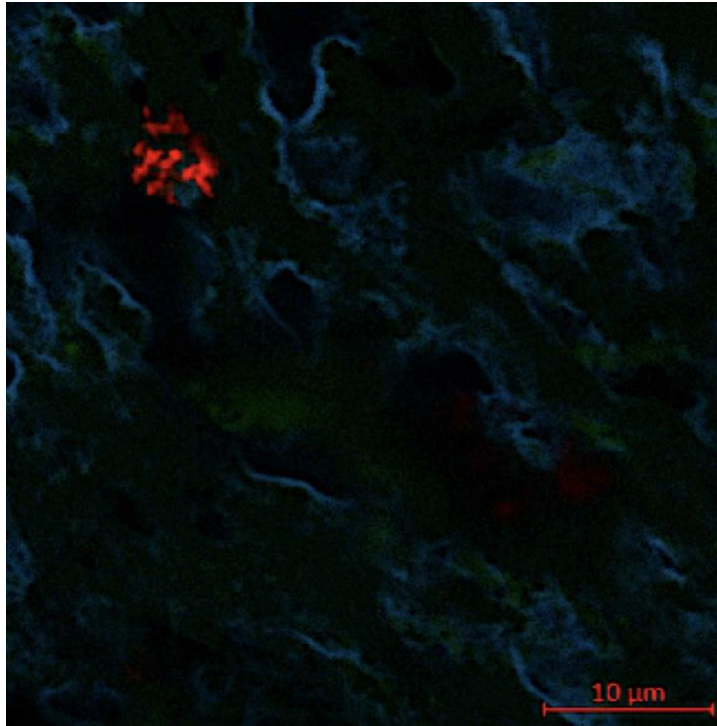
f. Sample P_6. Diffuse aggregates of coccid and rod-shaped cells.



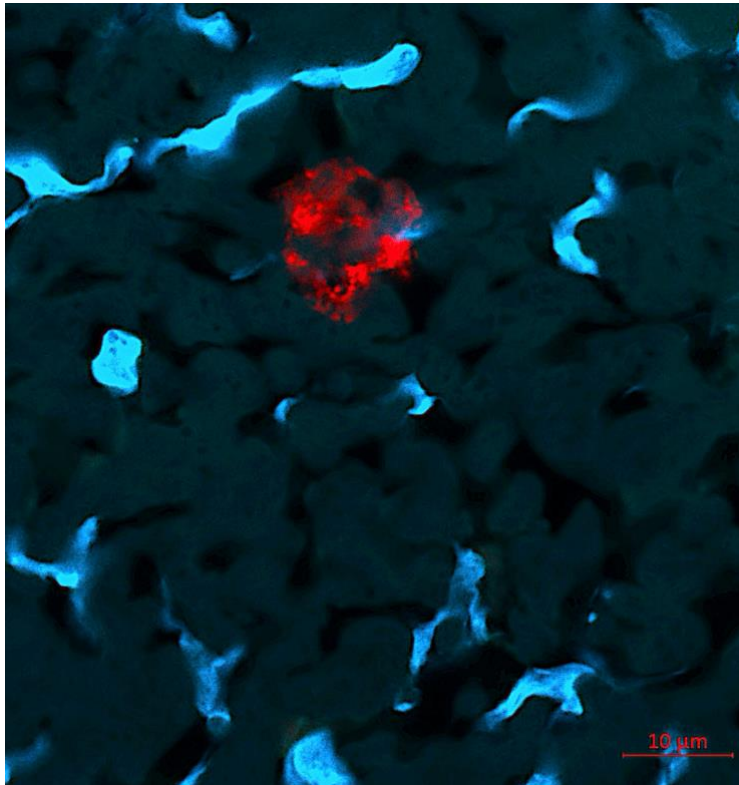
g. Sample P_9. Dense aggregate of coccid and rod-shaped cells surrounded by planktonic microorganisms



h. Sample P_10. White arrow shows a small aggregate of coccid cells top left.



i. Sample P_11. Small aggregate of coccoid cells



J. Sample P_7. Aggregate of coccoid cells.

